FEATURES OF TRANSFORMATION OF THE MINERAL PARAGENETIC ASSEMBLAGES FROM COPPER SULFIDE ORES OF THE KRASNOV HYDROTHERMAL FIELD (16°38' N Mid–Atlantic Ridge)

Nadezhda N. Mozgova
Institute of Geology of Ore Deposits, Petrography, Mineralogy, and Geochemistry RAS Moscow, Russia, mozgova@igem.ru
Yury S. Borodaev
Geology Department, Lomonosov Moscow State University, Moscow, Russia
Irina F. Gablina
Geological Institute, Russian Academy of Sciences, Moscow, Russia
Tamara V. Stepanova
All-Russia Research Institute for Geology and Mineral Resources of the World Oceans, St. Petersburg, Russia
Georgiy A. Cherkashev
All-Russia Research Institute for Geology and Mineral Resources of the World Oceans, St. Petersburg, Russia
Tat'yana Yu. Uspenskaya
Shirshov Institute of Oceanology, Russian Academy of Sciences, Moscow, Russia

Copper sulfide ores of the 5—80 thousands age from the Krasnov relic hydrothermal field (16°38' , Mid-Atlantic Ridge) have been studied with optical microscope, electron microscope equipped with energy dispersion system (SEM-EDS), electron microprobe, and X-ray diffraction.
According to the mineralogy, three types of paragenetic assemblages are recognized. Type I is homogeneous isocubanite with Cu-rich sulfides (bornite and copper sulfides of the chalcocite-digenite series). Type II is exsolved isocubanite and its unique products of subsequent transformation. Type III is oxide-sulfate-sulfide, which is characterized by iron specialization and is divided into two subtypes: with predominant pyrite (IIIa) and with predominant Fe-Cu sulfates and Fe oxides (IIIb). Type III contains relics of the highly modified type II paragenesis. The age relationship of type I has not been established.
6 tables , 8 figures, 23 references.

General review of the Krasnov hydrothermal ore field

The new hydrothermal field at 16°38' N of the Mid-Atlantic Ridge (MAR) was discovered in 2004 by the Polar Marine Geosurvey Expedition and All-Russia Research Institute for Geology and Mineral Resources of the World Ocean, (St. Petersburg, Russia) during Cruise 24 of the R/V *Professor Logachev*. During a subsequent voyage in 2006, this field was extended and was named Krasnov in honor of Sergei Gelievich Krasnov (1952-1996), a marine geologist, who investigated oceanic hydrothermal mineralization for the last 15 years of his brilliant professional career. Brief information on geology, zoning and mineralogy of ores was previously reported by Bel'tenev *et al.* (2006).

The Krasnov ore field, located in the eastern margin of the rift valley at a depth of 3700—3760 m is confined to the junction zone of the axial rift rise and the slope of the rift valley and is controlled by the intersection of the nearmeridian deep margin fault and the sublatitudinal fault. Approximately 60% of the bottom surface, which was studied with teleprofiling is covered by carbonate sludge up to 160 cm thick. Two sulfide ore bodies of 370 x 580 m and 110 x 130 m in size occur over the outcrops of primary basalts and occur as fine and medium blocks and relics of sulfide mounds covered by sediments and red crusts.

Sulfide bodies are composed mainly of pyrite; copper and copper massive sulfide ores are less abundant and zinc massive sulfide ores are practically absent. According to texture and morphology, massive, porous, and veinlet-impregnated ores, as well as ores of the chimney complex were defined in the ore field. In addition to massive sulfides, the ore-bearing sediments with Fe > 10% and Cu + Zn > 0.25% occurred as a band 30—150 m wide north and northeast of Orebody 1, and are found within the ore field. Pyrite, atacamite, aragonite, chalcocite, native copper, hematite, barite, and Fe

and Mn hydroxides were identified in these sediments.

The high oxidation of the ores, weak anomalies of metals content in dissolved and suspended phases in water samples, as well as the absence of hydrothermal fauna, indicate the relict nature of the ore field, of which the hydrothermal activity has actually terminated. This is confirmed by the dating of sulfide ores; the U/Pb age determined for 16 samples ranges within 5−80 kyr (Kuznetsov *et al.*, 2007). Iron specialization, continuance of formation, and the presence of sedimentary cover differentiate this field from the other hydrothermal fields within the Mid-Atlantic Ridge.

According to Bel'tenev *et al.* (2004), the ore types and major minerals were recognized as a result of the initial mineralogical and geochemical studies of the new field. The aim of this study is to provide more detailed textural, structural, and chemical investigation of ores from the chimney complex of the copper mineralization and to reveal the features of transformation of the mineral paragenetic assemblages in the hydrothermal field that is uncommon for this region.

Materials and experiments

Samples of the copper mineralization have been studied as the most interesting in terms of mineralogy and the easiest transformation due to the high mobility of copper. The samples occur as irregularly-shaped fragments containing copper minerals and are frequently covered by the black soot crust. Small pieces of these samples were fixed by epoxy to prepare polished sections (without heating).

After study under reflected light, microsamples and polished sections were investigated with a JEM-100C scanning electron microscope and a CamScan MX 2500S scanning electron microscope equipped with a Link-10000 energy dispersion system (accelerating potential 25 kV, current 0.4 nA) (SEM-EDS), Institute of Geology of Ore Deposits, Petrography, Mineralogy, and Geochemistry, Russian Academy of Sciences (IGEM RAS), Moscow and a CamScan MV2300 scanning electron microscope equipped with an energy dispersion system − INCA Energy 200, Geological Institute, Russian Academy of Sciences, Moscow. In the latter case, the utilized software requires the normalization procedure to 100% of the total elements recorded in spectrum. A number of analyses was performed with a Camebax SX-50 electron microprobe, Lomonosov Moscow State University. Accelerating potential was 20 kV, current, 30 nA. The following standards were used (Kα X-ray lines): FeS(Fe, S), CuS (Cu), ZnS (Zn). Most analyses were made with SEM-EDS since the low current allowed measurements of numerous points in the fine grains of minerals. Total analyses were about 500. X-ray study was performed with a Rigaku D/Max 2200 diffractometer, CuKα radiation in IGEM RAS and a RKD 57.3 camera (Fe radiation, 6 h exposure) in Fersman Mineralogical Museum, Russian Academy of Sciences, Moscow.

Mineralogy of the copper ores from the Krasnov field

Sulfides common for the oceanic ores from the Mid-Atlantic Ridge were identified in the studied samples. Isocubanite, chalcopyrite, and pyrite are the major minerals; bornite and copper sulfide are minor and sphalerite and marcasite are rare. Prevalence of idaite, Cu_3FeS_4, previously described from the submarine ores of the black smokers at 21° N East Pacific Rise (Oudin, 1983) and the presence of new phases of the Cu-Fe-S system with provisional names *X*, *Y*, and *M* are noticeable. In addition to sulfides, Fe-Cu sulfate and Fe oxides are important; quartz, opal, barite, and native sulfur are also abundant.

The size of studied sulfide grains ranges from 0.3−0.5 mm (occasionally up to 1 mm), but usually ranges from 1−2 to 50 μm. Diagnostics of the minerals have been performed by electron microprobe and SEM-EDS; in some cases, an X-ray diffraction study was applied. The representative data are given in Tables 1−6, in ternary plot Cu-Fe(Zn)-S (Fig. 1), and in photomicrographs of polished sections and microsamples (Figs. 2−8).

Isocubanite, the cubic analogue of rhombic cubanite, plays the most important role in the copper ores of Krasnov. Some explanations in regard to this mineral appear to be necessary. As a new mineral species, it was found for the first

Table 1. **Chemical composition of isocubanite (polished sections and microsamples)**

Anal.	Sample	Cu, wt.%	Fe	S	Total	Formula	Fig.
1**	1271-4	25.56	38.57	35.89	100.02	$Cu_{1.1}Fe_{1.9}S_{3.0}$	5d
2	1269-6/1	23.42	40.16	35.98	99.56	$Cu_{1.00}Fe_{1.95}S_{3.05}$	
3*	1269-6/1	23.09	42.27	35.29	100.65	$Cu_{0.98}Fe_{2.05}S_{2.97}$	
4*	1269-6/1	22.77	42.45	35.75	100.98	$Cu_{0.96}Fe_{2.04}S_{3.00}$	4d
5*	1269-6/2c	22.92	42.03	35.32	100.27	$Cu_{0.98}Fe_{2.04}S_{2.98}$	
6	1269-6/1	22.67	44.87	34.64	99.18	$Cu_{0.98}Fe_{2.06}S_{2.96}$	4b
7	1269-6/1	21.97	42.07	36.17	100.21	$Cu_{0.93}Fe_{2.03}S_{3.04}$	
8	1269-6/1	21.88	42.01	34.58.	98.47	$Cu_{0.95}Fe_{2.07}S_{2.98}$	4b
9	1271-4	21.34	42.57	36.26	100.17	$Cu_{0.91}Fe_{2.05}S_{3.04}$	7b
10*	1271-4	21.29	43.46	36.39	101.14	$Cu_{0.89}Fe_{2.08}S_{3.03}$	8c

Notices: * is EDS-SEM analysis, without *, is electron microprobe analysis. ** is microsample. Formula coefficients for phases analyzed in polished sections are accurate within two decimal digits, in microsamples, to one

Table 2. **Chemical composition of chalcopyrite and phase X (polished section and microsamples)**

Anal.	Sample	Cu, wt.%	Fe	S	Total	Formula	Fig.
					Chalcopyrite		
1*	1269-6/1	36.73	29.51	33.77	100.01	$Cu_{1.07}Fe_{0.98}S_{1.95}$	4a
2*	1269-6/1	35.21	30.69	34.09	99.99	$Cu_{1.02}Fe_{1..02}S_{1.96}$	
3*	1269-6/2c	34.50	31.17	34.33	100.00	$Cu_{1.00}Fe_{1..03}S_{1..97}$	4c
					Phase X		
4	1269-6/2c	33.12	35.58	34.72	103.42	$Cu_{0.93}Fe_{1.14}S_{1..93}$	
5	135-6/1	32.86	29.58	37.40	99.84	$Cu_{0.94}Fe_{0..96}S_{2.11}$	6a
6	1269-6/2c	32.54	35.42	33.64	102.12	$Cu_{0.93}(Fe_{1.15}Zn_{0..02})_{1.17}S_{1.90}$	3e
7	1269-6/2c	32.49	37.14	33.65	103.28	$Cu_{0.92}Fe_{1.19}S_{1..89}$	3e
8	1269-6/2c	31.41	31.76	35.41	98.58	$Cu_{0.91}Fe_{1..05}S_{2.04}$	
9*	1269-6/2c	31.20	32.64	34.66	98.50	$Cu_{0.91}Fe_{1..08}S_{2.01}$	
10*	1269-6/2c	30.98	34.18	34.37	99.53	$Cu_{0.90}Fe_{1.12}S_{1.98}$	
11	1269-6/2c	30.72	35.50	34.57	100.79	$Cu_{0.88}Fe_{1.16}S_{1.96}$	
12	135-6/1	32.41	33.10	33.96	99.99	$Cu_{0.94}(Fe_{1.09}Zn_{0.02})_{1.11}S_{1.95}$	6a
13**	1269-6/1	29.21	32.14	38.65	100.00	$Cu_{0.8}Fe_{1.0}S_{2.2}$	

Notices: 0.62 (anal. 6) and 0.47 (anal. 12) wt.% Zn

time in the oceanic ores (Caye *et al.*, 1988) and had previously been often described from continental and oceanic ores under different names including "chalcopyrrhotite" (Ramdohr, 1980; Oudin, 1983), "cubic cubanite" (Genkin *et al.*, 1966), "high cubanite" (Vaughan & Craig, 1978; Lebedev *et al.*, 1988). Despite the stochiometric formula $CuFe_2S_3$ listed in handbooks, isocubanite is attributed to the typical minerals with variable compositions and is commonly considered the natural analogue of the high-temperature intermediate solid solution (Iss) phase in the central part of the Cu-Fe-S system. In oceanic ores, exsolution textures of Iss are observed much more frequently than homogeneous crystals.

Isocubanite from the Krasnov field is not exceptional. It occurs as homogeneous grains and crystals, but usually plays the role of matrix in the exsolution textures of the higher-temperature isocubanite solid solution. The matrix comprises regular (most frequently latticed) intergrowths of lamellae of chalcopyrite and close phases and is often rimmed by diffused chalcopyrite. As shown below, these textures in Krasnov are characterized by the unique feature of subsequent strong transformations. According to analyses (Table 1), the chemical composition of isocubanite in examined samples ranges within limits (wt.%) 21.29–25.56 Cu, 38.57–44.87 Fe, and

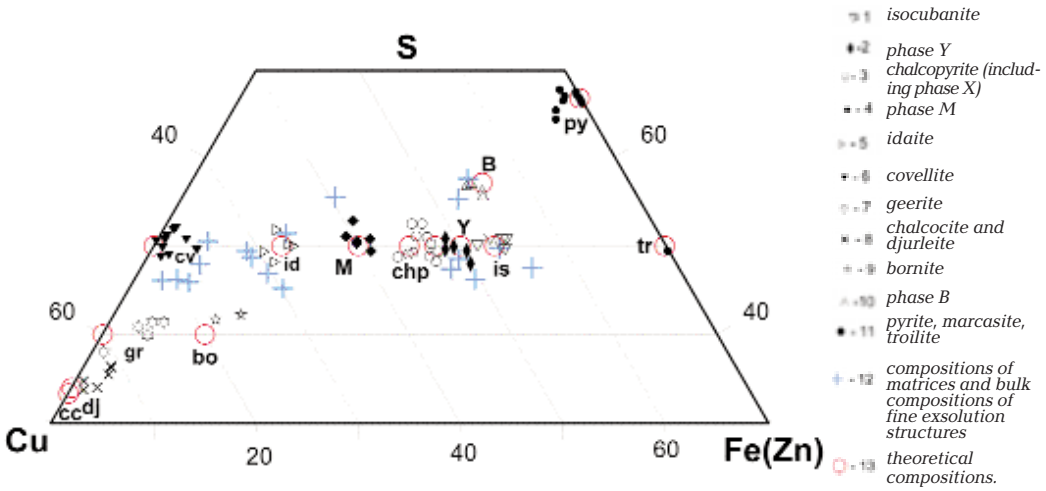

Fig. 1. The Cu-(Fe+Zn)-S ternary plot showing the distribution of chemical composition of the studied minerals (set of representative and averaged analyses is used; see Tables 1—5).
Abbreviations of minerals: isocubanite (Is), - chalcopyrite (Chp), idaite (Id), bornite (Bo), covellite (Cv), chalcocite (Cc), geerite (Gr), djurleite (Dj), pyrite (Py), marcasite (Mc), troilite (Tr); new phases (X, Y, M, B).

Table 3. **Chemical composition of idaite and new phases *Y*, *M*, and *B* (polished sections and microsamples)**

Anal.	Sample	Cu wt%	Fe	S	Total	Formula	Fig.
			Idaite, Cu_3FeS_4, calculated on the basis of 8 atoms				
1**	135-1b	53.18	13.23	33.59	100.00	$(Cu_{3.1}Fe_{0.9})_{4.0}S_{4.0}$	
2*	1269-6/1	52.35	15.06	32.57	99.08	$(Cu_{3.1}Fe_{1.0})_{4.1}S_{3.9}$	4b
3**	187-1/2	48.60	17.33	34.07	100.00	$(Cu_{2.9}Fe_{1.1})_{4.0}S_{4.0}$	
4*	1269-6/1	49.97	15.52	34.53	100.02	$(Cu_{2.94}Fe_{1.04})_{3.98}S_{4.02}$	
			Phase *Y* $Cu_2Fe_3S_5$ calculated on the basis of 10 atoms				
1**	1269-6/1	30.63	35.72	35.44	101.79	$Cu_{2.1}Fe_{2.8}S_{5.1}$	
2	1269-6/1	30.40	34.04	35.54	99.98	$Cu_{2.18}Fe_{2.77}S_{5.05}$	
3**	1269-4/2	29.95	35.16	36.50	101.61	$Cu_{2.1}Fe_{2.8}S_{5.1}$	
4*	1269-6/2c	28.66	35.65	34.82	99.13	$Cu_{2.07}Fe_{2.94}S_{4.99}$	4c
5	1289-6/2c	28.25	39.92	33.64	101.79	$Cu_{2.10}Fe_{2.82}S_{5.08}$	
6	135-6/1	28.81	36.09	33.82	100.00	$Cu_{2.08}(Fe_{2.97}Zn_{0.08})_{3.05}S_{4.85}$	
7	1269-6/2c	27.39	37.86	34.77	100.02	$Cu_{1.96}Fe_{3.09}S_{4.95}$	
8	135-6/1	30.45	36.10	32.79	100.01	$Cu_{2.21}(Fe_{3.00}Zn_{0.05})_{3.05}S_{4.74}$	6a
9	1269-6/2c	30.68	37.93	34.28	103.65	$Cu_{2.15}(Fe_{3.03}Zn_{0.05})_{3.08}S_{4.77}$	
			Phase *M* (Me_5S_5, $Cu_3Fe_2S_5$), calculated on the basis of 10 atoms				
1*	135-6/2a	42.27	22.16	35.56	99.99	$(Cu_{3.06}Fe_{1.83})_{4.89}S_{5.11}$	
2*	135-1/2c	40.61	22.16	37.22	99.99	$(Cu_{2.91}Fe_{1.81})_{4.72}S_{5.28}$	
3*	1269-6/1	40.31	26.28	34.62	101.21	$(Cu_{2.90}Fe_{2.16})_{5.06}S_{4.94}$	4d
4*	1269-6/1	41.26	23.81	34.91	99.98	$(Cu_{3.00}Fe_{1.97})_{4.97}S_{5.03}$	4d
5*	1269-6/1	41.14	23.76	35.12	100.02	$(Cu_{2.99}Fe_{1.96})_{4.95}S_{5.05}$	4d
			Phase *B* (Me_3S_4, $CuFe_2S_4$), calculated on the basis of 7 atoms				
1*	135-6/1	22.54	33.78	40.69	97.01	$Cu_{1.11}Fe_{1.90}S_{3.99}$	6c
2*	135-6/1	22.16	34.82	41.57	98.55	$Cu_{1.08}Fe_{1.92}S_{4.00}$	6c
3*	135-6/1	22.08	33.75	41.43	97.26	$Cu_{1.08}Fe_{1.89}S_{4.03}$	
4*	135-6/1	21.15	31.17	39.87	98.45	$Cu_{1.04}(Fe_{1.75}Zn_{0.30})_{2.05}S_{3.91}$	6b
5*	135-6/1	20.95	30.90	40.51	98.61	$Cu_{1.03}(Fe_{1.73}Zn_{0.30})_{2.03}S_{3.94}$	6b

Notices. Zn (wt.%) has been detected in phase *Y* 1.28 (anal. 6), 0.56 (anal. 8) and 0.76 (anal. 9); in phase *B*, 6.26 (anal. 4) and 6.25 (anal. 5); in the idaite item analyses 1 and 3 have been made with a CamScan MV2300 electron microscope.

Table 4. **Chemical composition of high Cu copper sulfides and bornite (polished sections, sample 135-1b)**

Number of anal.	Cu wt.%	Fe	S	Total	Formula	Fig.	Mineral
1*	78.68	1.26	20.06	100.00	$(Cu_{1.98}Fe_{0.04})_{2.02}S$	2a	Chalcocite
2*	77.44	1.38	20.54	99.36	$(Cu_{1.90}Fe_{0.04})_{1.94}S$		Djurleite
3*	76.66	2.60	20.74	100.00	$(Cu_{1.86}Fe_{0.07})_{1.93}S$		Djurleite
4*	74.71	2.81	22.48	100.00	$(Cu_{1.68}Fe_{0.07})_{1.75}S$		Digenite
5*	74.54.	2.92	22.37	99.83	$(Cu_{1.68}Fe_{0.08})_{1.76}S$		Digenite
6*	74.82	3.26	21.92	100.00	$(Cu_{1.72}Fe_{0.08})_{1.80}S$		Digenite
7*	75.82	2.60	21.58	100.00	$(Cu_{1.77}Fe_{0.07})_{1.84}S$		Roxbyite
8*	61.57	11.50	26.94	100.01	$Cu_{4.81}Fe_{1.02}S_{4.17}$	2b	Bornite
9*	58.19	14.00	27.34	99.53	$Cu_{4.54}Fe_{1.24}S_{4.22}$	2a	Bornite

Notice: All analyses (with the exceptions of 2, 7, and 8) were made with a CamScan MV2300 scanning electron microscope.

Table 5. **Chemical composition of covellite (Me/S ≈ 1) and geerite (series of low Cu copper sulfides) (polished sections and microsample)**

Number of anal.	Sample	Cu, wt.%	Fe	S	Total	Formula	Fig.
				Geerite			
1*	135-1b	75.11	1.19	23.70	100.00	$(Cu_{1.6}Fe_{0.03})_{1.63}S$	
2*	135-1b	70.64	3.37	25.99	100.00	$(Cu_{1.37}Fe_{0.07})_{1.44}S$	
3*	135-1b	69.82	4.90	25.28	100.00	$(Cu_{1.39}Fe_{0.11})_{1.5}S$	
				Cu-sulfide of the covellite series			
4*	135-1b	68.95	4.61	26.44	100.00	$(Cu_{1.32}Fe_{0.10})_{1.42}S$	
5*	135-1b	67.63	5.90	26.47	100.00	$(Cu_{1.29}Fe_{0.13})_{1.42}S$	
				Covellite			
6*	1271-4/3	67.60	0.31	33.39	101.30	$Cu_{1.02}S$	7a
7*	135-6/2a	64.61	0.85	34.54	100.00	$(Cu_{0.94}Fe_{0.01})_{0.95}S$	
8**	1269-4/2	64.08	1.64	32.16	97.88	CuS	
9*	135-6/2a	63.19	1.38	35.43	100.00	$(Cu_{0.9}Fe_{0.02})_{0.92}S$	
10**	135-1b	61.42	5.23	33.35	100.00	$(Cu_{0.9}Fe_{0.1})_{1.0}S$	

Notices: analyses 1–5, 7, 9, and 10 were made with a CamScan MV2300 scanning electron microscope.

34.58–36.39 S, which is close to the ranges of contents listed in the review on oceanic isocubanite (Mozgova *et al.*, 1995).

On the basis of the data given in the tables and figures, let us briefly characterize the other sulfides from our samples.

Along with lamellae and rims in exsolution textures, chalcopyrite is less frequently observed as grains and homogeneous crystals. Its chemical composition given in Table 2 ranges within the limits of (wt.%) 29.21–36.73 Cu, 29.51–35.58 Fe, and 33.64–38.65 S. These data include both compositions close to the stoichiometry and Fe-rich variety of this mineral, which was previously called phase *X* (Mozgova *et al.*, 2005). Diversion from stoichiometry is expressed by the approximate formula $Cu_{1-x}Fe_{1+x}S_2$, where x is most frequently about 0.1. Sporadically, an impurity of 0.*n* % Zn was identified.

Idaite, which is occasionally observed in the oceanic ores, therein is characterized by various morphologies. These are matrices, altered areas of lamellae, colloform zones, and even euhedral crystals. The chemical composition listed in Table 3 is as follows (wt.%): 48.60–53.18 Cu, 13.23–17.33 Fe, and 32.59–34.53 S.

Close to isocubanite phase *Y*, $Cu_2Fe_3S_5$, was discovered in the oceanic ores as lamellae within the isocubanite exsolution textures (Mozgova *et al.*, 2002), then described as homogeneous grains from Rainbow (Borodaev *et al.*, 2004), and is distinguished by the larger Cu/Fe value in comparison with isocubanite. Previously, such a stoichiometric compound was observed in mete-

orites (Rambaldi *et al.*, 1986). In the Krasnov field, this phase occurs as fine grains among weakly and highly altered products of the isocubanite exsolution, as well as euhedral crystals identified for the first time. Microprobe analysis with a unfocused beam of 15 x 15 μm of some grains within the exsolution texture revealed a bulk composition which corresponded to phase *Y*, implying that the exsolution of phase *Y* is similar to isocubanite when conditions change. The chemical composition of this phase listed in Table 3 ranges within the limits (wt.%): 27.39–30.68 Cu, 34.04–39.92 Fe, and 32.79–36.50 S. Zn occurs as an impurity varying from 0.56 to 1.28 wt.%.

Phase *M*, $Cu_3Fe_2S_5$, the intermediate between chalcopyrite and idaite (Fig. 1), was identified for the first time. It most frequently originated from the transformation of chalcopyrite lamellae leading to the distortion of their morphology; but locally, it is present within the altered matrix. The range of composition is as follows (wt.%): 41.14–42.27 Cu, 22.16–26.28 Fe, and 34.62–37.22 S (Table 3).

A new phase *B* that is richer in Fe and enriched in S in comparison with isocubanite was observed as zoned and zoned-colloform bands within the transformed isocubanite exsolution textures. The chemical composition of this phase given in Table 3 ranges within the limits (wt.%): 20.95–22.54 Cu, 30.90–34.82 Fe, and 39.87–41.57 S. Impurities of Zn – up to 6.26 wt.%, are frequent and are probably the result of adjacent grains of sphalerite.

Bornite and Cu-rich sulfides of the chalcocite-digenite series frequently occur as fine two-phase or polymineralic mixtures (Table 4). Sulfides depleted of Cu occur as the geerite-covellite series (Table 5). As shown below, they are different both in composition and type of assemblages. In some cases, diagnostics of the copper sulfides is provisionally because X-ray data, which are necessary for identification of nonstoichiometric sulfides, could not be collected due to tiny grains and fine intergrowths

It should be noted that the composition of all sulfides of the system of Cu-Fe-S occurred in a matrix of the exsolution textures has the most significant deviation from the ideal formulae of corresponding minerals and phases. It is evidently caused by extremely fine mechanical admixtures. In the compositional diagram (Fig. 1), these data are marked by blue crosses.

Pyrite, marcasite, and troilite are the examined iron sulfides. Pyrite is characterized by diverse morphologies, such as skeletal pseudomorphs after pyrrhotite crystals, single euhedral crystals, irregular-shaped grains, branchy aggregates, and rims around grains with an exsolution texture. Subordinate marcasite is included in pseudomorphs after pyrrhotite and occurs as irregular-shaped grains and fine rims around branchy pyrite. The impurity of copper (0.03–4.76 wt. %) is frequently detected in the iron disulfides, but their compositions are usually close to stoichiometry. Troilite was observed in only one polished section as small inclusions in goethite. Its composition is close to stoichiometry as follows (wt.%): 64.04 Fe, 35.96 S; formula is $Fe_{1.01}S_{0.99}$.

Sphalerite was observed as euhedral crystals and rims around grains with the exsolution texture structure of the isocubanite solid solution. The content of iron in this mineral ranges from 13.22 to 16.08 wt.% with an average value of 14.84 wt.%.

Paragenetic types of sulfides

As a result of this study, three types of paragenetic assemblages were recognized:

- **Type I** is homogeneous isocubanite and Cu-rich copper sulfides of the chalcocite-digenite series. Age relationship with other types was not revealed.
- **Type II** is exsolved isocubanite and the products of its diverse and unique transformations.
- **Type III** is an oxide-sulfate-sulfide, which in contrast to the two other types is characterized by the iron specialization and is divided into two paragenetic subtypes: with predominant pyrite (IIIa) and with predominant Fe-Cu sulfates and Fe oxides. Type III contains relics of the highly transformed type II paragenetic assemblages.

Paragenetic type I, comprising homogeneous isocubanite, bornite, and Cu-rich copper sulfides, is not abundant in the studied samples. Bornite, chalcocite, and nonstoichiometric sulfides of the chalcocite-digenite series are developed metasomatically in isocubanite along different oriented cracks and form

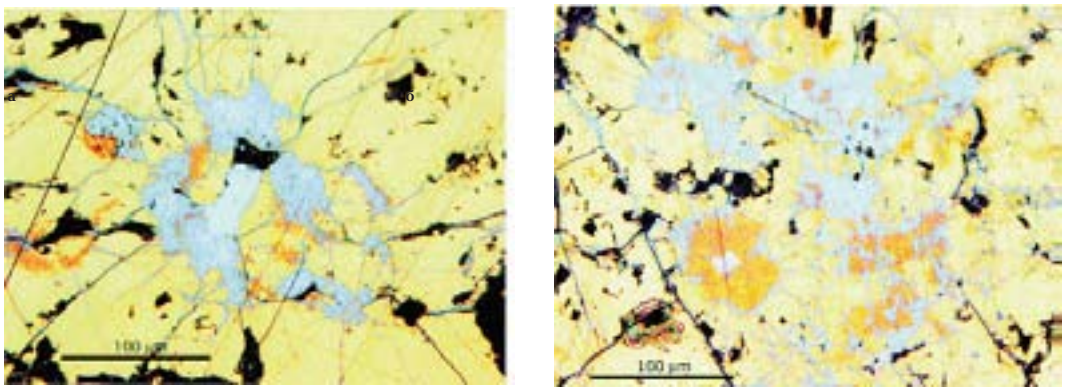

a b

Fig. 2. Type I sulfide assemblages presented by bornite and Cu-rich copper sulfides. Polished sections under reflected light. Sample 135-1b.
(a) Thin metasomatic veinlets and nests of bornite (orange), chalcocite (bluish gray), and a mixture of the Cu-rich sulfides of the chalcocite-digenite series (blue, heterogeneous) in homogeneous isocubanite. Chalcocite (Table 4, anal. 1) surrounded by sulfides depleted in copper occurs in the central parts of nests and veinlets; bornite (Table 4, anal. 10) originates at the contact between the Cu-poor sulfides and isocubanite. (b) The same assemblage in the neighboring areas, where in the left lower part of photomicrograph, the chalcocite core (Table 5, anal. 1) within round nest which is surrounded by bornite (Table 4, anal. 9),which in turn is surrounded by the copper sulfides (Table 4, anal. 7). In the other places, the veinlets of copper sulfide cut bornite and contain its relics.

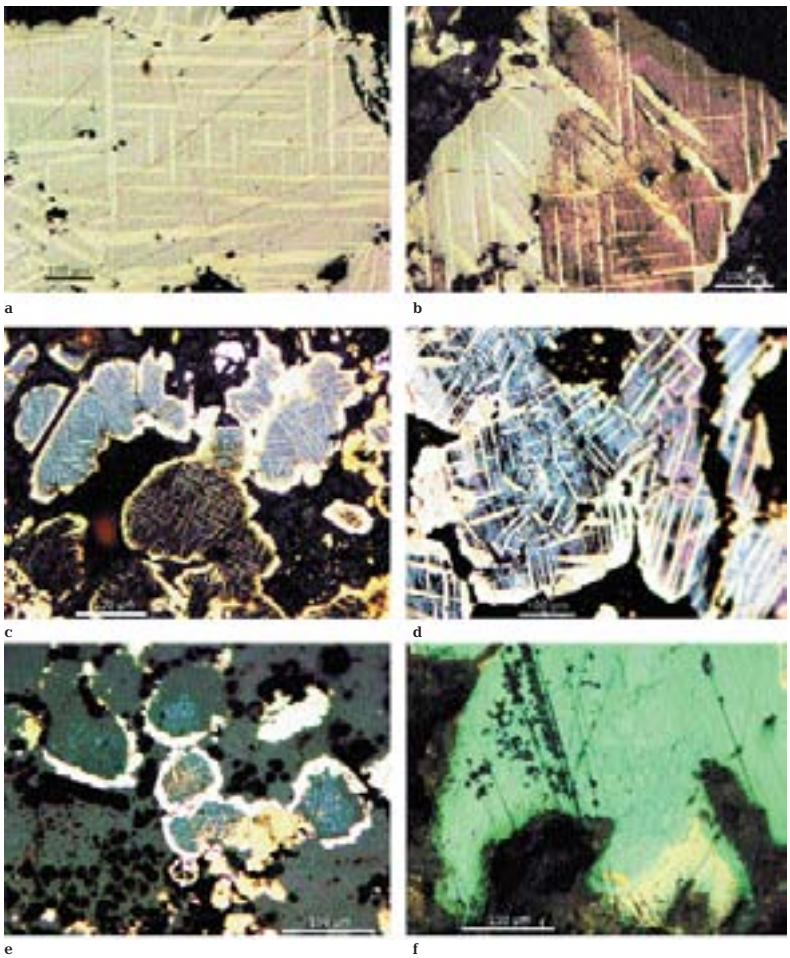

a b c d e f

Fig. 3. Type II sulfide assemblages presented by exsolved isocubanite with different color of matrix. Polished sections under reflected light.

(a) Exsolution texture with untransformed light beige matrix and lattice of chalcopyrite lamellae. Sample 135-6/2.

(b) Grain with untransformed light beige matrix and transformed brown matrix. Sample 135-6/2.

(c) Segregation of grains with bluish gray and black matrices with lamellae and rims of chalcopyrite. Sample 1269-6/2c.

(d) Segregation of grains with blue and pinkish matrices with lamellae and rims of chalcopyrite. Sample 135-6/2.

(e) Olive matrix in exsolution texture with rims of pyrite (white) and Fe-rich chalcopyrite (light yellow) (Table 2, rim (anal. 6), lamellae (anal. 7)). Sample 1269-6/2c.

(f) Fine flake segregations of covellite (blue) after Cu-poor copper sulfides (greenish gray); covellite metasomaticaly replaces the isocubanite exsolution texture; light relict of untransformed texture in the lower part of photomicrograph. Sample 135-6/1.

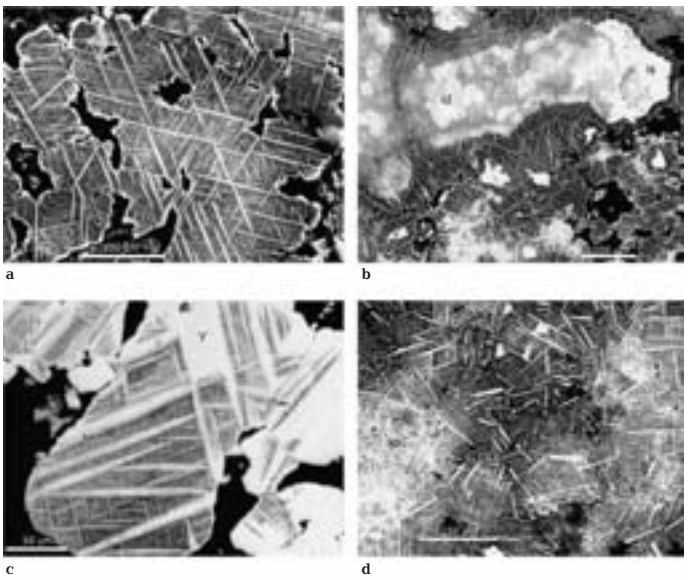

Fig. 4. BSE images of latticed textures in transformed matrices of the exsolved isocubanite and the newly formed sulfides in them. Polished sections.

(a) Black covellite-bearing matrix with two systems of lamellae and rims of chalcopyrite (Table 2, anal. 1) around pores. Sample 1269-6/1.

(b) Elongate heterogeneous grain with grayish white fuzzy spots of the newly formed idaite (id) and phases close to it (Table 3, anal. 2) against the background of the latticed exsolution texture with black matrix in the light "head" of the grain, which is newly formed isocubanite (is) (Table 1, analysis 6). Sample 1269-6/1.

(c) Large lamellae of chalcopyrite (Table 2, anal. 3) with traces of transformation are superimposed on the net of fine lamellae in the dark matrix. Locally, phase Y (Table 3, anal. 4) is developed after the matrix between the lamellae with partial trapping of the latter. Sample 1269-6/c

(d) Different oriented large lamellae of phase M deviated from squared shape (Table 3, analyses 3–5) are superimposed on fine exsolution texture with black matrix; minute white grains between the large lamellae are the newly formed isocubanite (Table 1, anal. 4). Sample 1269-6/1.

branchy thin veinlets and nests in the intersections of the latter. On the basis of the Me/S ratio, among copper sulfides, chalcocite, djurleite, digenite, and roxbyite were identified. Only chalcocite and djurleite were confirmed by X-ray diffraction study.

As shown in Fig. 2a, relationships between bornite and copper sulfides are unambiguous. On the one hand, bornite (Table 4, anal. 8) directly contacting with isocubanite surrounds veinlets and pods of the copper sulfides, with the replacement of bornite by a heterogeneous mixture of Cu sulfides derived from the veinlets. Chalcocite occurs in the central parts both of veinlets and pods. On the other hand, in some pods, bornite alternates with Cu sulfides in the zoned structures. Figure 2b demonstrates that the chalcocite grain is surrounded by bornite (Table 4, anal. 8), which in turn is rimmed by copper sulfides (Table 4, analysis 7). Frequently, veinlets of copper sulfides intersect bornite and contain its relics.

Paragenetic type II occurs as exsolution textures of the high-temperature isocubanite and products of their transformations are predominant in the examined samples and are characterized by a number of specific features.

First of all, the relationships of lamellae within matrices indicate the complexity of the exsolution. In addition to the lattices consisting of the blades of one generation, the juxtaposition of two or more different oriented systems is observed; lamellae of these systems are different in morphology and size (Figs. 3a, 4a). These evidently argue multiple exsolutions and the variable dynamics of this process.

The unique features of the isocubanite exsolution texture in the Krasnov field are various marks of succeeding strong transformations. The change of the matrix color is the most demonstrative feature. In the "fresh" unmodified textures, the matrix is light beige under reflected light (Fig. 3a). However, more frequently, due to metasomatic replacement with the later minerals, the matrix is brown, gray, blue, and olive, ranging to black (Figs. 3b-g). Often, the color changes within a single grain (Fig. 3b), with lamellae remaining without modifications.

The chemical composition of the replaced matrices (Tables 1-5, Fig. 1) demonstrates that coloration is caused by replacement minerals: grayish brown matrices are close to phase *Y* in composition, light brown, to phase *B*, dark brown, to phase *M*, much darker brown, to idaite, blue, to Cu-poor sulfides of the covellite series; sulfates were identified in a dark gray matrix and mixtures with covellite, in a black one. The elevated contents of sulfur in comparison with the formula indicate an admixture of sulfates.

During further transformations, the newly

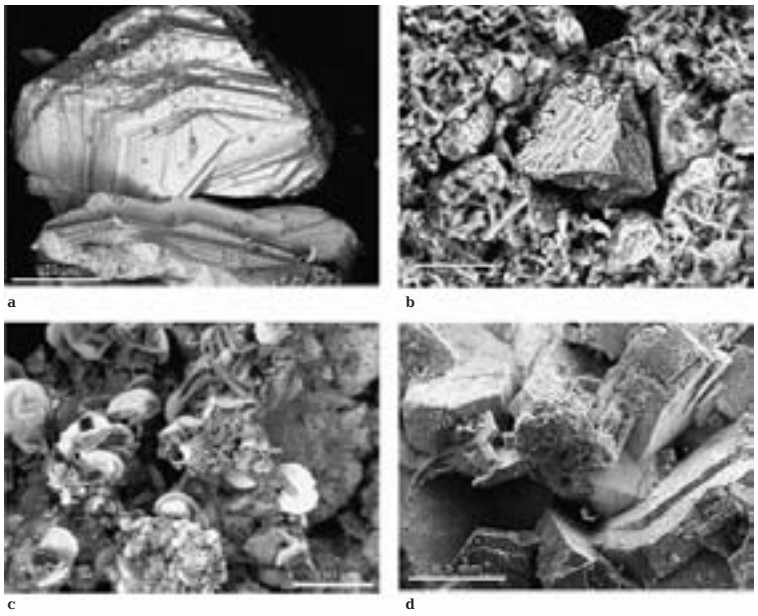

Fig. 5. BSE images of crystals of the newly formed sulfides among the secondary products. Microsamples.
(a) Intergrowths of the lamellar isocubanite crystals (Table 1, anal. 1) with the rare fine powder of pyrite and copper sulfides on faces. Sample 1271-4.

(b) Crystal of phase Y among exsolution products of isocubanite. Sample 1269-6/1.

*(c) Crystals of covellite (white, Table 4, anal. 8) partially with the crust of copper and iron sulfate among the secondary products. Sample 1269-4/2**.*

(d) Crystals of marcasite with powder of copper sulfides (probable pesudomorph after pyrrhotite). Sample 187-1/2.

formed homogeneous phases appear against the background of selected replacement matrices. These phases are nearly all Cu-Fe and Cu sulfides, as well as their mixtures added by sulfates and oxides of the same metals (unfortunately, study of these mixtures failed because of their small size).

According to morphology, color and chemical composition, the following newly formed minerals and phases were identified:

1. Thin whitish (bluish under reflected light) spots with sporadic light clusters, which are spread on the transformed dark matrix and lamellae. The composition of such spots and clusters is close to idaite (Table 3, anal. 2) within elongated grains (Fig. 4b) hosted in the exsolution texture with black covellite-bearing matrix. At the same time, the denser newly formed homogeneous isocubanite (Table 1, anal. 6, 8) is observable in the host matrix. The black matrix and lamellae of the primary exsolution texture appear through the whitish spots, whereas they are not observed in the dense isocubanite grains.

2. The homogeneous light grains developed after the transformed matrix between lamellae and partially trapping the latter or "spilling" along the contact. For example, the newly formed phase *Y* (Fig. 4c; Table 3, anal. 4) replaces the areas of dark matrix between the large lamellae of chalcopyrite (Table 2, anal. 3). These lamellae in turn are juxtaposed on the frame of small lamellae, which were also transformed.

3. The small newly formed generations modify the composition and distort the shape of host chalcopyrite lamellae. Such transformed lamellae correspond to phase *M* in composition (Fig. 4d; Table 3, anal. 3-5) and accompany the appearance of the above mentioned whitish spots.

4. Well-shaped crystals of sulfides appear among extremely transformed products of the isocubanite exsolution on the surface of microsamples (Figs. 5a-d). They occur as segregations of homogeneous isocubanite with the fine powder of copper sulfides and pyrite or as different sulfides, which are involved in the transformation of exsolution products. Presence of homogeneous isocubanite crystals among the modified exsolution products of high-temperature generations of this mineral clearly proves the neoformation of these crystals.

Further transformation of the exsolved isocubanite results in the conversion to the lattice-type structure. The juxtaposition of rounded phenocrysts of chalcopyrite (Table 2, anal. 5) on the very fine latticed exsolution texture with a bulk composition close to phase *Y* (Table 3, anal. 8) transforms this texture to nearly impregnated one (Fig. 6a). Fine grains with practically indistinguishable lattice are occasionally transformed into colloform and zoned structures (Figs. 6b, 6c). The new phase *B* occurred as thin zones (Table 3, anal. 4, 5) in the

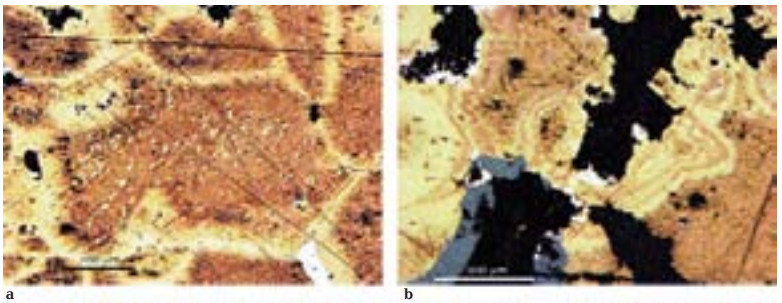

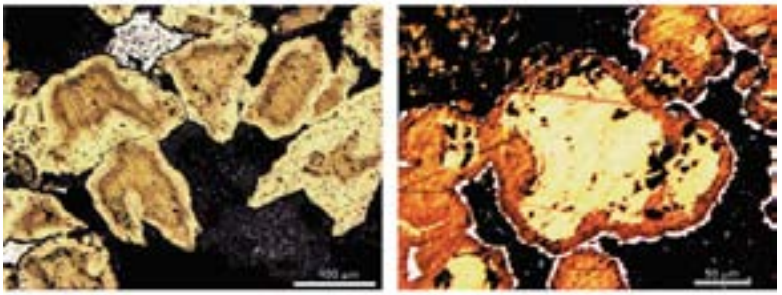

Fig. 6. Transformation of exsolution texure of isocubanite. Sample 135-6/1. Photomicrographs of polished sections under reflected light.

(a) Oriented rounded phenocrysts of chalcopyrite (Table 2, anal. 5) is superimposed on the very fine light brown exsolution texture of phase Y (Table 3, analysis 8) with the chalcopyrite rim.

(b) Colloform segregation developed after the isocubanite exsolution texture with light zones of new phase B (Table 3, anal. 4, 5); in the left lower corner, sphalerite is dark gray band and cavities are black.

(c) Zoned texture formed at transformation of isocubanite: fine heterogeneous sulfide-sulfate cores with dark rims dominated by sulfates are surrounded by the light zones of new phase B (Table 3, anal. 1, 2). Relief grain of pyrite is in the upper part of the photomicrograph.

(d) Light grain of isocubanite with dark heterogeneous sulfide-sulfate rim and outer rim of pyrite (white).

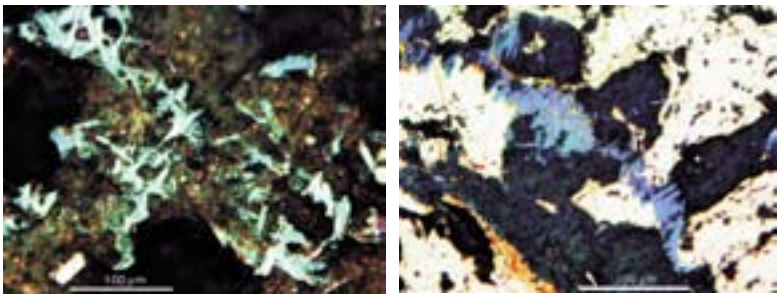

Fig. 7. Segregation of late covellite. Photomicrographs of polished sections under reflected light.

(a) Intergrowths of sheet-like covellite crystals with clearly pronounced bireflectance (from blue to bluish gray) (Table 5, anal. 6) in fine-grained sulfide-oxide mass. White grain in the left lower corner is pyrite. Sample 1271-4/3.

(b) Veinlet of blue sheet-like crystals of covellite in isocubanite (Table 1, anal. 9). Locally, crystals of covellite are outlined by thin rim of newly formed chalcopyrite. Sample 1271-4.

colloform areas and margins (Table 3, anal.1, 2) of zoned grain and was observed solely in such structures. In the newly formed zoned textures, the heterogeneous sulfate segregations with different locations are also observable. For example, in Fig. 6c, the thin dark zone enriched in sulfate separates the sulfate-sulfide core from the light outer band of phase *B*, whereas in Fig 6d, sulfates occur as a broad zone along the margins of the isocubanite grain and are outlined by an outer thin rim of pyrite. In some cases, the primary texture of the isocubanite solid solution completely disappears at the zone of dense metasomatic replacement, both of lamellae and matrix by the grained Cu-poor copper sulfides with fine-flake segregations of early covellite (see Fig. 3f). The later coarse lamellar covellite is associated with the sulfate-oxide segregations (Fig. 7a) and cut through homogeneous isocubanite (Fig. 7b).

It should be emphasized that the mineral assemblages that are exsolution products of isocubanite, subsequent to their transformation, are prevalent in the Krasnov field and are observed for the first time.

The oxide-sulfate-sulfide paragenetic type III is significantly different from the two mentioned above by its iron specialization and is divided into two subtypes: with predominant pyrite (a) and with predominant Cu-Fe sulfates and Fe

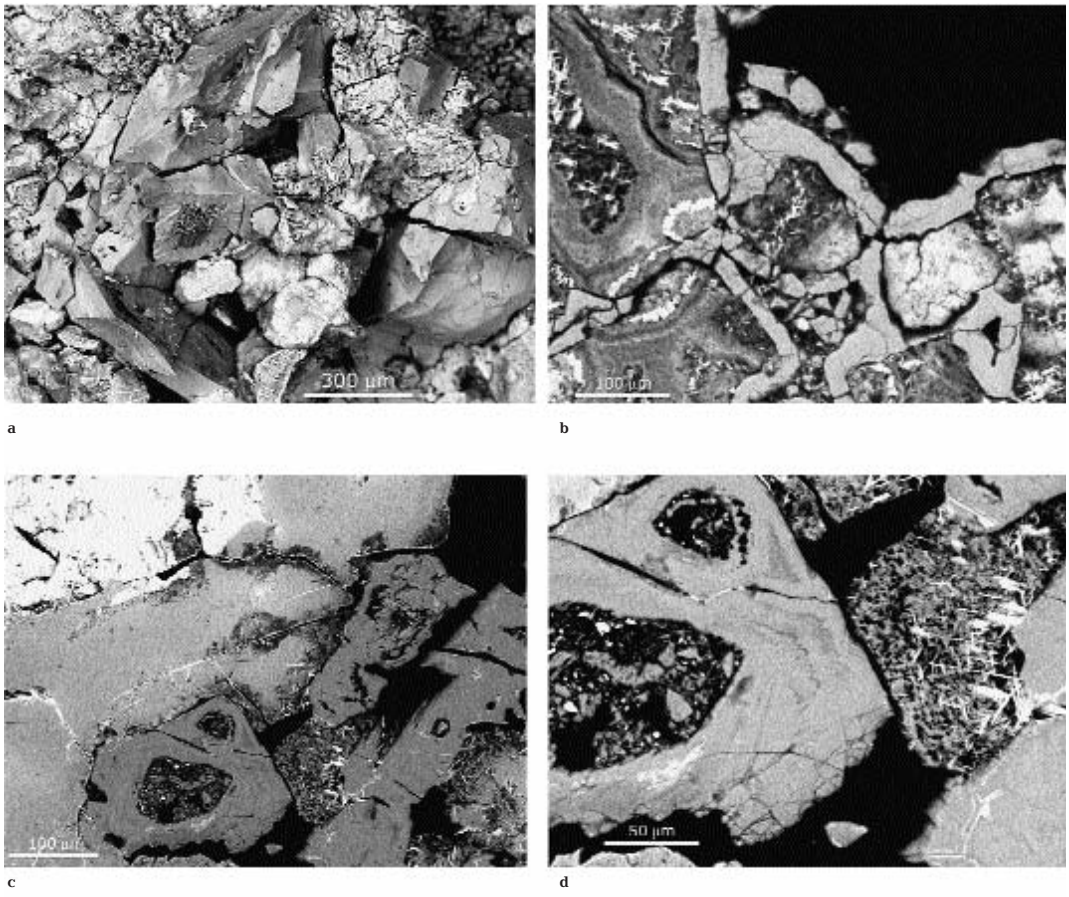

Fig. 8. Type III of paragenetic assemblages is oxide-sulfate-sulfide.

(a) BSE image of microsample. Sample 187-1/2. (b-d) Photomicrographs of polished sections under reflected light. Sample 1271-4. (a) Desintegrated area of ore on the piece surface presented by relic grains with the traces of highly transformed latticed exsolution texture surrounded by the larger fragments of pyrite.

(b) Breccia-like structure with broad rims of Cu-bearing pyrite around the highly transformed heterogeneous ore fragments. The lightest and coarse-grained zone in colloform area of fragment is a phase close to idaite. The other white grains are unidentified Cu-Fe sulfides enriched in sulfur (probably due to surrounding sulfates).

(c) Assemblage of goethite (relief isometric dark-gray grains of subtile-zoned structure) and Cu-Fe sulfate (light gray in centre) in contact with homogeneous isocubanite (white, in the left upper corner, Table 1, anal. 10); thin veinlet-like segregations in sulfates and goethite are syngenetic sulfides; the highly transformed fragment of the type II assemblage is between grains of goethite; two rounded cavities with microbreccia of dissolution (contains grains of goethite and sporadic sulfides) are in isometric goethite grain.

(d) Detail of the same photomicrograph. In the isometric goethite grain, light veinlet-like segregations concordant to zoning of goethite are composed of troilite. The other sulfides are not identified. Highly transformed fragment displays the latticed structure, where portions of lamellae were converted to the idaite-like phase.

oxides (b). In regard to type II, type III formed later, because it contains only relics of grains with extremely transformed latticed textures.

An example of paragenesis with predominant late pyrite (subtype a) is shown in Figs. 8a and 8b, where it is observed within extremely disintegrated and brecciated areas of ores, which host the most modified primary exsolution textures of isocubanite. These textures in relic fragments are frequently transformed to colloform-zoned areas (Fig. 8b), where separated thin zones are composed of the newly formed Cu-Fe sulfides close to idaite in composition. These newly formed sulfides are assumed to be formed nearly simultaneously with surrounding pyrite.

An example of oxide-sulfate paragenesis

with subordinate sulfides (subtype b) is shown in Figs. 8c and 8d. Goethite and sulfate close to natrojarosite are the predominant minerals. Goethite (α-FeOOH) occurs as gray relief grains with thin-zoned texture and deep red inner reflections. Analysis was confirmed by chemical composition (wt.%): 52.99 Fe, 4.85 Cu, 36.73 O, 1.98 S, and 0.96 Cl, total is 97.31 and X-ray diffraction pattern with the following strongest reflections (Å): 4.195(9), 2.715 (10), 2.434 (9), 2.217 (7), and 2.718 (4).

In comparison with goethite, the sulfate grains are lighter and in lower relief. Proximity to natrojarosite is indicated by the X-ray powder pattern collected from the material extracted from the analyzed sample (Table 6). However, according to electron microprobe data, this sulfate contains (wt.%) 39.60 Fe, 19.86 Cu, 30.98 O, 10.43 S, 0.85 Cl, total is 101.87; copper occurs instead of sodium and the Fe/S atomic ratio exceeds that which is typical of jarosite (2 as opposed to 1.5) (the composition of natrojarosite is calculated from the theoretical formula $NaFe_3(SO_4)_2(OH)_6$ and is as follows (wt.%): 34.57 Fe, 4.74 Na, 46.21 O, 13.23 S, 1.25 H).

The Cu-Fe sulfate from the Krasnov field is not excluded from being a new mineral species (or variety) of the alunite group and further examination is needed. In any case, incorporation of the smaller copper ion instead of sodium probably explains the decreasing of some d-spacings in the studied sulfate in comparison to the standard values of natrojarosite. In this connection, it may be noted that the wide range of the Fe/S value even in individual minerals is given in the last review on sulfates. For example, in schwertmannite discovered in 1994 with the ideal formula $Fe_8O_8(OH)_{8-2x}(SO_4)_x.nH_2O$, where $1 \leq x \geq 1.75$, the Fe/S ratio ranges from 8 to 4.6 indicating intermediate composition between goethite and jarosite (Bigham & Nordstrom, 2000).

In polished sections (Figs. 8c, 8d), the sulfate segregation borders on the homogeneous isocubanite at one margin (Table 1, anal. 10) and slightly corrodes this mineral and at the other margin, on goethite, but in the latter case, their relationship is masked by very fine branchy black segregations developed after sulfate in the near-contact area. Along cut cracks, these segregations penetrate into isocubanite. They are similar in morphology to fine-acicular aggregates of schwertmannite reported in the above cited paper, where jarosite and goethite are described as common members of the schwertmannite assemblages.

Table 6. **Comparison of X-ray powder pattern for Cu-Fe sulfate and standard X-ray patterns of natrojarosite**

Sample 1271-4		PDF # 110302		PDF # 301203	
I	*d*	*I*	*d*	*I*	*d*
		40	5.94	30	5.94
		50	5.57	40	5.57
6	5.00	100	5.06	90	5.06
		20	3.67	30	3.66
7	3.46	20	3.49	20	3.49
		70	3.12	90	3.12
10	3.06	80	3.06	100	3.06
		20	2.960	20	2.960
4	2.746	20	2.780	30	2.783
4	2.536	40	2.530	30	2.527
				10	2.308
1	2.245	60	2.240	50	2.236
2	2.087	20	2.130		
3	1.928	60	1.980	50	1.979
4	1.905	5	1.910	30	1.909
5	1.856			10	1.857
		50	1.830	50	1.834
		5	1.740	20	1.743
7	1.714	5	1.720	20	1.724
				5	1.693
				5	1.657
3	1.602			20	1.623
5	1.583	20	1.570	20br	1.578
		20	1.540	20	1.560
				30	1.532
		20	1.480	10	1.484
5	1.453	40	1.479	40br	1.479
1	1.311	5	1.340		
1	1.198				
3	1.072				

The grains of goethite and sulfate contain thin veinlet-like segregations of simultaneous Fe sulfides concordant to the zoning of goethite. Troilite has been identified in one such veinlet. Two oval cavities with the microbreccia of dissolution are observed in the goethite grain as traces of the later effect. Fragments within these cavities mainly present the same goethite with the sporadic grains of

sulfides. The chain of fine goethite grains arranged along the wall of the smaller cavity follow its morphology (Fig. 8d).

In the polished section (Fig. 8d), an "alien" component is relict of highly transformed primary exsolution texture in the cavity between the goethite grains. The latticed structure of the relict nearly disappeared and the residual thickened lamellae were converted to the idaite-like phase.

Taking into account the relationship between type II and type III paragenetic assemblages, the latter is suggested to finalize the subordinate copper mineralizing process and signal the transition to the pyrite ores, which are predominant in the Krasnov hydrothermal field.

Discussion

The results obtained display the specific character of the mineral paragenetic assemblages of the copper ores at Krasnov.

Briefly described type I paragenetic assemblages, where isocubanite does not exsolve are similar to the mineral assemblages from the youngest active sulfide chimneys in the Rainbow hydrothermal field ($36^0$14' N, Mid-Atlantic Ridge), which were studied in detail (Bogdanov *et al.*, 2002; Borodaev *et al.*, 2004; Mozgova *et al.*, 2005). The sulfide mineralogy in these chimneys is nearly identical to the type I paragenetic assemblages in the Krasnov field and phase *Y*, that is close to isocubanite preserves as homogeneous. Despite the small dimensions of cut veinlets, in most cases, the mineral distribution is similar to that in the Rainbow chimneys: bornite in contact with isocubanite alternates with the heterogeneous copper sulfides toward the center of the veinlet (or nest), where chalcocite, the Cu-richest sulfide of this assemblage, occurs. Taking into account the Mössbauer data on Cu and Fe valances in the examined sulfides (Vaughan & Craig, 1978), the major steps of the transformation are as follows: isocubanite $Cu^{+}Fe^{2+}Fe^{3+}S_2 \rightarrow$ bornite $Cu^{+}{}_5Fe^{3+}S_4 \rightarrow$ chalcocite $Cu^{+}{}_2S$. These metasomatic conversions appear to be caused by increasing oxidation, potentially due to the effect of sea water penetrating along fissures. As a result of this, iron is oxidized and removed and minerals are enriched with the remaining copper. Some deviations from this scheme (for example, indications of zoning) are due to the dynamic environment during the formation of this assemblage. It should be added that the increased oxidation potential does not reach the levels that were documented in the young Rainbow chimneys where chalcocite is replaced with minerals depleted in Cu. By analogy with Rainbow, this type can be assumed to have been derived from the sufficiently high-temperature short-lived source.

Similar schemes reflect some common features of the Cu-Fe-sulfide transformation. In particular, it is consistent with the documented supergene alteration of these minerals at continental deposits (Sillitoe & Clark, 1969; Constantinou, 1975; Large *et al.*, 1995).

The much more abundant type II, which is related to the exsolution texture of isocubanite, is characterized by indications of the subsequent transformations. First of all, these are multiple repetitions of exsolution that indicate the violent dynamics and high temperature of the initial stage of the copper ore formation, since the thermal stability of isocubanite is $\geq 200^{\circ}$C (Vaughan & Craig, 1978).

Resulting heterogeneity of the matrix in the exsolution products can explain another feature of these paragenetic assemblages that is widespread, the unique selective replacement of the matrix. The involvement of different minerals in this process is apparently due to localized conditions, which vary depending upon the decreasing of temperatures and the increasing of the oxidation potential. As a result, replacement minerals and phases become Fe-poorer and are enriched in Cu (see compositions on the line with Me/S = 1 in Fig. 1) and in some cases, sulfates are developed separately after the matrix.

The further transformation results in newly formed homogeneous minerals and phases of the Cu-Fe-S system incorporated in modified matrices and lamellae in the exsolution textures. The presence of non-exsolved isocubanite among the newly formed phases as grains and homogeneous crystals indicates an increase of temperature that can be caused by renewed fluid influx. The appearance of the metastable phases, which were observed neither in nature nor experiment under equalibrium is noteworthy. According to terminology suggested by F.V. Chukhrov, such phases may be defined as

"ephemer-minerals". The reason for their appearance "is the rapid chemical reactions that prevent the formation of stable phases" (Chukhrov, 1973). They are easily converted under change of conditions that contribute to the transition of the exsolution textures to other structural-textural generations change.

In this type of paragenetic assemblages, most minerals are identified as Cu-Fe and Cu sulfides, involved in all stages of the isocubanite exsolution texture transformation: from the metasomatic replacement of the matrix at an early stage, through the newly formed phases, to the formation of cut veinlets at the latest stage. It can be emphasized that the presence of Cu-poor sulfides (covellite $Cu^{2+}S$ and related nonstoichiometric sulfides) in this paragenetic type, and Cu-rich sulfides in type I, testify to the more oxidizing conditions of transformation for type II.

In the type III assemblages, the subtype with predominant late pyrite cementing highly transformed fragments of the isocubanite exsolution textures apparently indicates an influx of new portions of hot fluids enriched in Fe.

Goethite and poorly studied Cu-Fe sulfate that is intermediate between the jarosite family and schwertmannite in the Fe/S ratio are the major minerals of the oxide-sulfate subtype. According to the recent reviews (Bigham & Nordstrom, 2000; Dutrizac & Jambor, 2000; Jambor *et al.*, 2000), goethite and Fe sulfate of the jarosite family, the most common components of oxidized zones of massive sulfide deposits, also occur in hypogene settings. Hypogene jarosite is documented in hot springs of Yellowstone National Park in the USA, crater lake of the Mendeleev volcano in the Kunashir Island, Kurily and other similar localities. A.A. Godovikov reported (1983) that hypogene jarosite is uncommon and is not abundant. As a secondary mineral, it is metasomatically developed after nearly all iron minerals due to the oxidizing of the latter (Ramdohr, 1980).

The relationships of minerals described from our samples of the oxide-sulfate paragenetic assemblages contribute to the hypogene origin of these minerals, because the features of high replacement of primary Cu-Fe sulfides with these minerals are absent and the minerals contain fine segregations of simultaneous Fe sulfides (including troilite, FeS; although, Fe-monosulfides are absent in the other paragenetic types). Any interaction between the type III paragenetic assemblage and relics of the greatest transformed primary assemblage was not observed (see Fig. 8d).

Comparison of the data obtained allows the following conclusion. The type I paragenetic assemblages not in contact with the other types may be considered by analogy with the Cu chimneys from Rainbow as young mineralizations formed for the short period which appears to explain their weak transformation. Predominant paragenetic type II of the highest transformed assemblages is most probably related to the oldest and long-lived source. Iron assemblages of type III accomplish the deposition of Cu-Fe ores and are transitional to the major pyrite stage of mineralization in this field. The alternation of the geochemical specialization of fluids is probably the result of modifications in the ore-forming system.

Thus, the study of the transformation of the copper-bearing paragenetic assemblages (some of which are unique) from the Krasnov field show the complex nature of the mineralizing processes in this area and gives additional information on oceanic mineralization.

Acknowledgements

We thank I.A. Bryzgalov, N.V. Trubkin, L.A. Livitskaya, L.A. Pautov, N.V. Gor'kova, and A.T. Savichev for their assistance in instrumental investigations and personnel of the Polar Marine Geosurvey Expedition for the ore samples kindly placed at our disposal. We are grateful to E.A. Borisova and S.N. Nenasheva for discussion and helpful advices.

This study was supported by the Russian Foundation for Basic Researches (project no. 05-05-64952).

References

Bel'tenev, V.E., Shagin, A.A., Markov, V.F., Rozhdestvenskaya, I.I., Lazareva, L.I., Fedorov, I.P., Cherkashev, G.A., Stepanova, T.V., Poroshina I.M. & Shilov, V.V. (**2006**): New hydrothermal ore field at 16°38' N of the Mid-Atlantic Ridge // Dokl. Russ. Acad., Sci. Earth Sci. Sec. 408, 530 – 534.

Bigham, J.M. & Nordstrom, D.K. (**2000**): Iron and aluminum hydroxysulfates from acid sulfate

waters // In: Rev. Mineral. Geochem. Mineral. Soc. Amer. Washington 40, 351–403.

Bogdanov, Yu.A., Bortnikov, N.S., Vikent'ev, I.V., Lein, A.Yu., Gurvich, E.G., Sagalevich, A.M., Simonov, V.A., Ikorskii, S.V., Stavrova, O.O. & Apollonov, V.N. (**2002**): Mineralogical-geochemical peculiarities of hydrothermal sulfide ores and fluids in the Rainbow field associated with serpentinites, Mid-Atlantic Ridge // Geol. Ore Dep. 44(4), 444–473.

Borodaev, Yu.S., Mozgova, N.N., Gablina, I.F., Bogdanov, Yu.A., Starostin, V.I. & Fardust, F. (**2004**): Zoned chimneys of black smokers from the Rainbow hydrothermal field // Moscow University Geology Bulletin, 59(3), 44–62 (in Russ.).

Caye, R., Cervelle, B., Cesbronm, F. et al. (**1988**): Isocubanite, a new definition of the cubic polymorph of cubanite $CuFe_2S_3$ // Miner. Mag. 52, 509–514.

Chukhrov, F.V. (**1973**): Ephemeral minerals // Priroda (9), 64–69 (in Russ.).

Constantinou, G. (**1975**): Idaite from the Skouriotissa massive sulfide orebody, Cyprus: its composition and conditions of formation //Amer. Mineral. 60, 1013–1018.

Genkin, A.D., Filimonova, A.A., Shadlun, T.N, Soboleva, S.V. & Troneva, N.V. (**1966**): On cubic cubanite and cubic chalcopyrite // Geol. Ore. Dep. no. 1, 41–54 (in Russ.).

Godovikov, A.A. (**1983**): Mineralogy. Moscow, Nedra (in Russ.).

Dutrizac, J.E. & Jambor J.L. (**2000**): Jarosites and their application in hydrometallurgy // In: Rev. Mineral. Geochem. Mineral. Soc. Amer. Washington 40, 405–452.

Jambor, J.L., Nordstrom, D.K. & Alpers, C.N. (**2000**): Metal-sulfate salts from sulfide mineral oxidation // In: Rev. Mineral. Geochem. Mineral. Soc. Amer. Washington 40, 303–350.

Kuznetsov, V.Yu., Cherkashev, G.A., Lein, A.Yu., Bel'tenev, V.E., Maksimov, F.E., Shilov, V.V., Stepanova, T.V., Chernov, S.B., Baranova, N.G. & Tarasenko, D.I. (**2007**): Age of hydrothermal ores from Mid-Atlantic Ridge (according to Th^{230}/U dating) // Vestn. St. Petersburg Univ. Ser. 7, no. 2 (in Russ.).

Large, D.J., MacQuaker, J., Vaughan, D.J., Sawlowicz Z &, Gize A.P. (**1995**): Evidence for low-temperature alteration of sulfides in the kupferschiefer copper deposits of Southwestern Poland // Econ. Geol. 90, 2143–2155 .

Lebedev, L.M., Cherkashev, L.M., Tsepin, A.I. (**1988**): New data on mineralogy of sulfide ores from Atlantis II depression, Red Sea // In: Modern hydrothermal fluids and mineralization. Nauka, Moscow (110–123) (in Russ.).

Maslennikova, S.P. (**2005**): Sulfide pipes of Paleozoic black smokers, Yaman-Kasy and Alexandrov massive sulfide deposits, South Urals. Unpub. PhD thesis. Mineral. Inst. Urals Division, Russ. Acad. Sci., Miass (in Russ.).

Mozgova, N., Borodaev, Yu., Cherkashev, G., Stepanova, T. & Zhirnov E. (**2002**): High-temperature exsolution structures in submarine serpentinite-related massive sulfides (Mid-Atlantic Ridge). Minerals of the Ocean // Proc. Inter. Conf. St. Petersburg, Russian Federation, 134–137.

Mozgova, N.N., Borodaev, Yu.S., Gablina, I.F., Cherkashev, G.A. & Stepanova, T.V. (**2005**): Mineral assemblages as indicators of the maturity of oceanic hydrothermal mounds // Lithol. Mineral. Resour. 40, 293–319.

Mozgova, N.N., Nenasheva, S.N., Borodaev, Yu.S. & Tsepin, A.I. (**1995**): Field of composition and features of isomorphic substitution in isocubanite // Geokhimiya no. 4, 533–552 (in. Russ.).

Oudin E. (**1983**): Hydrothermal sulfide deposits of the East Pacific Rise. (21). Part I: Descriptive mineralogy // Marine Mining. N 4. P. 39–72.

Rambaldi E.R., Rajan R.S., Housley R.M., Wang D. (**1986**): Gallium-bearing sphalerite in a metal-sulfide nodule of the Qingzhen (EH3) chondrite // Meteoritics. V. 21. N 1. P. 23–31.

Ramdohr, P (**1980**): The ore minerals and their intergrowths. Pergamon Press, New York.

Sillitoe R.H., Clark A.H. (**1969**): Copper and copper-iron sulfides as the initial products of supergene oxidation, Copiapó mining district, northern Chili // Amer. Mineral. 54, 1684–1710.

Vaughan, D.J. & Craig, J.R. (**1978**): Mineral Chemistry of Metal Sulfides. Cambridge University Press, London.